

Chandra HIGH-RESOLUTION X-RAY SPECTROSCOPY OF THE Fe K LINE IN THE SEYFERT 1 GALAXY NGC 3783

T. Yaqoob^{a b}, J. N. Reeves^{a b c}, A. Markowitz^{b d}, P. J. Serlemitsos^b, and U. Padmanabhan^a

^a*Department of Physics and Astronomy, Johns Hopkins University, Baltimore, MD 21218.*

^b*Laboratory for High Energy Astrophysics, NASA/Goddard Space Flight Center, Greenbelt, MD 20771.*

^c*Universities Space Research Association.*

^d*N.A.S./N.R.C. Research Associate*

Abstract

We report on the results of detailed X-ray spectroscopy of the Fe-K region in the Seyfert 1 galaxy NGC 3783 using the *Chandra* High Energy Grating Transmission Spectrometer (*HETGS*). There were five observations over an interval of ~ 125 days in 2001, each with an exposure time of ~ 170 ks. The combined data constitute the highest signal-to-noise Fe-K spectrum having the best velocity resolution in the Fe-K band to date (FWHM ~ 1860 km s $^{-1}$). The combined data show a resolved Fe K α line core (FWHM = 1700^{+410}_{-390} km s $^{-1}$) with a center energy of 6.397 ± 0.003 keV, consistent with an origin in neutral or lowly ionized Fe, located between the BLR and NLR, as found by Kaspi *et al.* (2002). We also find that excess flux around the base of the Fe K α line core can be modeled with either a Compton scattering “shoulder” or an emission line (with about the same flux as the line core) from a relativistic accretion disk, having an inclination angle of 11° or less. This disk line model is as good as a Compton-shoulder model for the base of the Fe K α line core. In the latter model, we measured the column density to be $7.5^{+2.7}_{-0.6} \times 10^{23}$ cm $^{-2}$, which corresponds to a Thomson optical depth of ~ 0.60 , so the line-emitting matter is not quite Compton-thick. An intrinsic width of 1500^{+460}_{-340} km s $^{-1}$ FWHM is still required in this model. Moreover, more complicated scenarios involving both a Compton-shoulder and a disk line cannot be ruled out. We confirm an absorption feature due to He-like Fe (FWHM = 6405^{+5020}_{-2670} km s $^{-1}$), found in previous studies.

Keywords: accretion disks – galaxies: active – line: profile – X-rays: galaxies

To appear in the Astrophysical Journal, 10 July 2005

1. INTRODUCTION

At least part of the Fe K α fluorescent emission line in type I active galactic nuclei (AGNs) is believed to originate in a relativistic accretion disk around a black hole (e.g. see reviews by Fabian *et al.* 2000; Reynolds & Nowak 2003). The dominant peak energy of the Fe K α line at ~ 6.4 keV appears to be ubiquitous and this core of the line carries a substantial fraction of the total line flux (e.g. Nandra *et al.* 1997; Sulentic *et al.* 1998; Lubiński & Zdziarski 2001; Weaver, Gelbord, & Yaqoob 2001; Yaqoob *et al.* 2002; Perola *et al.* 2002; Reeves 2003; Yaqoob & Padmanabhan 2004). It has been traditional to associate such narrow Fe K α lines with an origin in distant matter, at least several thousand gravitational radii from the putative black hole (e.g. the optical broad-line region (BLR), the putative obscuring torus, or the optical narrow-line region (NLR)). However, Petrucci *et al.* (2002) recently reported a *variable*, narrow Fe K α line in

Mkn 841, supporting an accretion-disk origin (see also Longinotti *et al.* 2004). Moreover, rapidly variable, narrow Fe K line emission has been observed in the Seyfert I galaxy NGC 7314 (Yaqoob *et al.* 2003a). Thus, even narrow Fe K α lines may have a significant contribution from the accretion disk (Lee *et al.* 2002; Yaqoob *et al.* 2003a; Longinotti *et al.* 2004; Turner, Kramer, & Reeves 2004).

NGC 3783 is a fairly bright ($F_{2-10 \text{ keV}} \sim 5 - 7.5 \times 10^{-11}$ ergs s $^{-1}$), moderate luminosity ($L_{2-10 \text{ keV}} \sim 1 - 1.5 \times 10^{43}$ ergs s $^{-1}$), nearby ($z = 0.00973$) Seyfert 1 galaxy which has been well-studied in all wavebands. In the X-ray band, NGC 3783 was the target of the deepest observation with the *Chandra* high energy grating transmission spectrometer (*HETGS*) for any Seyfert galaxy, during a campaign in 2001, obtaining a net exposure time of ~ 830 ks. The spectra from this campaign represent the highest spectral resolution data with the best signal-to-noise for any

Table 1
Core Fe K Line *Chandra* (HEG) Spectral Fitting Results

Observation	E^a (keV)	I^b	EW ^c (eV)	FWHM ^d (km s ⁻¹)	F^e L^e
NGC 3783(1)	$6.401^{+0.008}_{-0.008}$ (6.390 – 6.412)	$4.77^{+1.31}_{-1.17}$ (3.22 – 6.58)	75^{+21}_{-18} (51 – 103)	2320^{+1225}_{-995} (990 – 4055)	5.0 1.1
NGC 3783(2)	$6.393^{+0.008}_{-0.009}$ (6.380 – 6.403)	$5.42^{+1.39}_{-1.22}$ (3.82 – 7.33)	85^{+22}_{-19} (60 – 115)	2545^{+1300}_{-915} (1365 – 4415)	5.1 1.1
NGC 3783(3)	$6.394^{+0.005}_{-0.005}$ (6.387 – 6.401)	$5.19^{+1.20}_{-1.08}$ (3.77 – 6.83)	81^{+19}_{-17} (59 – 107)	1205^{+940}_{-1205} (0 – 2540)	5.2 1.1
NGC 3783(4)	$6.396^{+0.005}_{-0.005}$ (6.389 – 6.402)	$5.61^{+1.25}_{-1.15}$ (4.08 – 7.31)	66^{+15}_{-14} (48 – 86)	1255^{+760}_{-1255} (0 – 2305)	7.4 1.6
NGC 3783(5)	$6.401^{+0.007}_{-0.006}$ (6.392 – 6.411)	$3.86^{+1.13}_{-1.02}$ (2.52 – 5.39)	51^{+15}_{-13} (33 – 71)	1345^{+990}_{-1345} (0 – 2715)	6.1 1.3
Total	$6.397^{+0.003}_{-0.003}$ (6.393 – 6.401)	$4.90^{+0.55}_{-0.52}$ (4.21 – 5.64)	70^{+9}_{-7} (60 – 80)	1700^{+410}_{-390} (1180 – 2250)	5.8 1.2

Chandra HEG data, fitted with a power law plus Gaussian Fe K α emission-line model in the 2–7 keV band (see §3). The purpose of these fits is primarily a *comparison* of the Fe K α emission-line parameters (see Fig. 3, Fig. 4, and Fig. 6 for more complex fits). Absolute values of the line intensity are model-dependent but the peak energy and width of the Fe K α line core are insensitive to the continuum and absorption model. The last row gives measurements from the summed spectrum (with ~ 830 ks exposure time), as derived in Yaqoob & Padmanabhan (2004). All fit parameters are quoted in the source rest frame. Line widths are *intrinsic*, since they have already been corrected for the instrumental line-response function. Statistical errors are for three interesting parameters and correspond to the 68% confidence level (ΔC -statistic = 3.51), whilst parentheses show the 90% confidence level ranges of the parameters (ΔC -statistic = 6.25). ^a Gaussian line center energy. ^b Emission-line intensity in units of 10^{-5} photons cm⁻² s⁻¹. ^c Emission line equivalent width. ^d Full width half maximum, rounded to 5 km s⁻¹. ^e F is the estimated 2–10 keV observed flux in units of 10^{-11} ergs cm⁻² s⁻¹ using the complex disk-line model in §6. The power-law continuum was extrapolated to 10 keV. L is the estimated 2–10 keV source-frame luminosity (using the 2–10 keV estimated flux), in units of 10^{43} ergs s⁻¹, assuming $H_0 = 70$ km s⁻¹ Mpc⁻¹, $\Omega_{\text{matter}} = 0.3$ and $\Omega_{\Lambda} = 0.7$.

Seyfert galaxy available to date. The observing campaign was also designed to study variability and was broken up into five observations separated by various intervals ranging from days to months. The soft X-ray part of the *HETGS* data has been well-studied by several research groups and has produced a wealth of new information and insights into the photoionized outflow and its variability (Kaspi *et al.* 2001, 2002, Netzer *et al.* 2003, Krongold *et al.* 2003). These results have been supplemented by studies using *XMM-Newton* (Behar *et al.* 2003; Reeves *et al.* 2004), and by studies in the UV band (e.g. Gabel *et al.* 2003a,b). On the other hand, the high-spectral resolution *HETGS* data for the Fe K α

line in NGC 3783 from the extended campaign in 2001 have not yet been fully exploited. Kaspi *et al.* (2002) reported measurements of the narrow core of the Fe K α line and detection of a Compton-scattering “shoulder” on the red-side of the core, indicating an origin for the line core in cold, optically-thick matter, far from the nucleus (beyond the optical BLR). Results of variability studies of the Fe K α line from within the extended observation campaign in 2001 have not yet been reported. A detailed study of the Fe K α line in NGC 3783 using *XMM-Newton* was presented by Reeves *et al.* (2004) who confirmed the *Chandra* measurements of the narrow core, and in addition reported that a broad, relativistic disk line

was not required by the data (a similar conclusion was reached by Kaspi *et al.* (2002) for the *Chandra* HETGS data).

In this paper we specifically study the Fe K α line in detail in NGC 3783 using the *Chandra* HETGS data from the extended campaign in 2001. We study the time-averaged spectrum, as well as the individual spectra from the five observations from the campaign in order to address line variability. We find that a Compton shoulder model is not a unique description of the complexity in the Fe K α line. A relativistic disk line model provides as good a fit as the Compton shoulder model. In §2 we describe the data and observations. In §3 we discuss the results of spectral fitting to derive parameters for the Fe K α line core, from the time-averaged spectrum as well as from the separate observations. In §4 we confirm the detection of an Fe He-like absorption feature. In §5 and §6 we describe the results of fitting a Compton shoulder model and relativistic disk-line model respectively, to the excess flux at the base of the core of the Fe K α line. Finally, we present our conclusions in §7.

2. OBSERVATIONS AND DATA

NGC 3783 was monitored over a period of ~ 125 days, starting 2001 February 24, with the *Chandra* HETGS during five snapshots. We will refer to these snapshots as observations (1) to (5). HETGS consists of two grating assemblies, a High-Energy Grating (HEG) and a Medium-Energy Grating (MEG), and it is the HEG that achieves the highest spectral resolution. The MEG has only half of the spectral resolution of the HEG and less effective area in the Fe-K band, so our study will focus on the HEG data. The *Chandra* data were reduced and HEG spectra made exactly as described in Yaqoob *et al.* (2003b). We used only the first orders of the grating data (combining the positive and negative arms). The mean HEG count rates ranged from 0.36 – 0.50 ct/s. The exposure times for observations (1) to (5) were in the range 165–169 ks. The count rate and exposure time for the total time-averaged HEG spectrum were 0.36 ct/s and 832 ks respectively. Background was not subtracted since it is negligible over the energy range of interest (e.g. see Yaqoob *et al.* 2003a). Note that the systematic uncertainty in the HEG wavelength scale is $\sim 433 \text{ km s}^{-1}$ ($\sim 11 \text{ eV}$) at 6.4 keV

¹.

Fig. 1 shows the 2–7 keV lightcurves for the five observations, showing the count rates summed over the -1 and $+1$ orders of both the MEG and the HEG, binned at 1024 s. It can be seen that the observations, each of duration ~ 2 days, were designed to probe timescales of ~ 1 day and less, $\sim 1, 2, 3$, and 4 weeks, 3 months, and 4 months. The 2–7 keV continuum variability over the first ~ 2 weeks of the campaign was confined to the flux remaining within $\sim \pm 25\%$ of the mean during that period, but in observation (4), about a month into the campaign, the overall flux was higher than the mean in the first two weeks of the campaign by $\sim 50\%$ (see Fig. 1). However, the variability about the new mean flux during observation (4) was still $\sim \pm 30\%$ relative to the mean in observation(4). In the final observation the 2–7 keV flux began back at its level at the beginning of the campaign, but by the end of the ~ 2 day observation it had risen by $\sim 50\%$, compared to the level at the beginning of final observation of the campaign. The excess variance above the expectation for Poisson noise (e.g. Turner *et al.* 1999), calculated over the entire ~ 4 month monitoring period from the lightcurve in Fig. 1 is $(4.52 \pm 0.28) \times 10^{-2}$.

3. SPECTRAL FITTING RESULTS

We used XSPEC v11.2 (Arnaud 1996) for spectral fitting. Since we were interested in utilizing the highest possible spectral resolution available, we used spectra binned at 0.0025 \AA , and this amply over-samples the HEG resolution (0.012 \AA FWHM). The C -statistic was used for minimization. By definition, calculation of the C -statistic requires only knowledge of the number of counts in a bin, but for spectral plots, the error bars shown correspond to asymmetric errors calculated using the approximations of Gehrels (1986). All model parameters will be referred to the source frame, unless otherwise noted. Note that since all models were fitted by first folding through the instrument response before comparing with the data, the derived model parameters *do not* need to be corrected for instrumental response.

¹<http://space.mit.edu/CXC/calib/hetgcal.html>

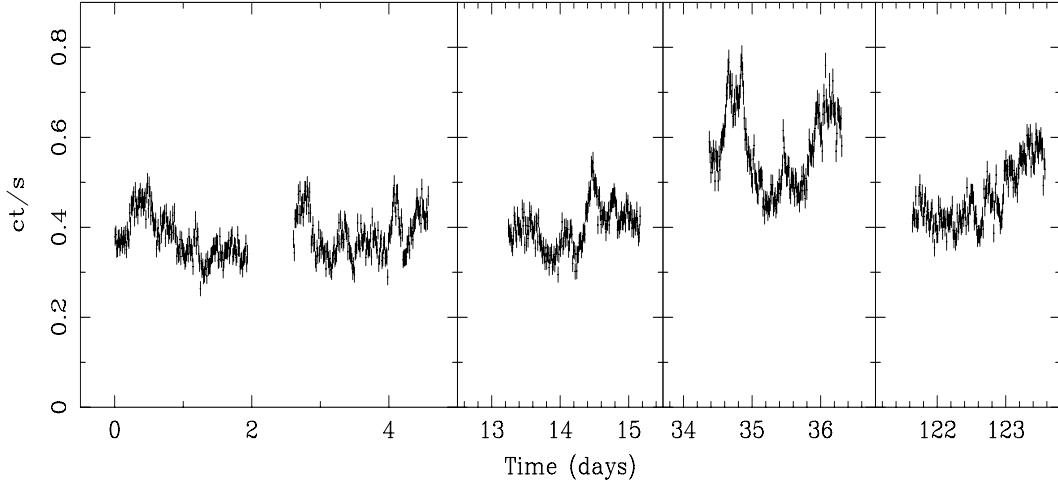


Figure 1. Lightcurves from the *Chandra* high-energy grating (*HETGS*) monitoring campaign of NGC 3783. In this paper, the five snapshots are referred to as observations (1)–(5). The first panel shows the first *two* snapshots, and the remaining three panels show one snapshot in each panel. Shown are the 2–7 keV count rates combined from MEG and HEG data, utilizing both the -1 and $+1$ orders of the gratings, binned at 1024 s. The zero reference time in this composite lightcurve is UT 2001 February 24 19:06:15. The scale on the time axis is such that equal lengths correspond to equal time intervals.

3.1. Simple Continuum Model

Our method is first to fit a simple empirical model to the continuum and extract parameters for the core of the Fe $K\alpha$ emission line to establish whether there is any intra-observation variability of the line parameters. Since we are *comparing* line parameters, and the line core is narrow (see YP04), this is good enough to guide subsequent, more detailed analysis. Accordingly, we will then describe more physical (and more complex) models for the continuum and absorption and show the extent of the sensitivity of the absolute parameters of the Fe $K\alpha$ emission-line core to details of these models.

Thus, we fitted a simple power law plus Gaussian emission-line model over the 2–7 keV band for each of the five spectra. The Gaussian component had three free parameters (line center energy, width, and intensity) so the model had five free parameters in total, including the continuum slope and normalization.

Although the Fe $K\alpha$ line consists of two components ($K\alpha_1$ and $K\alpha_2$, separated by 13 eV), we modeled it as a single Gaussian, since it was shown in Yaqoob *et al.* (2001), that with the spectral resolution of the HEG, there is a negligible impact on the measured line width. Some broadening may also result from the presence of line emission from more than one ionization state of Fe. However, we will bear this in mind when in-

terpreting the measured FWHM velocities. Also, the use of a single Gaussian (without any attempt to model the underlying broad Fe $K\alpha$ emission) has a negligible impact on the measured center energy of the core (see §6 and Yaqoob *et al.* 2001). In any case, we will compare the parameters obtained from the simple model with those obtained from more complex models (see §3.2, §5, and §6).

The best-fitting emission-line parameters for each spectrum are shown in Table 1 (as well as extrapolated 2–10 keV fluxes and luminosities obtained using more complex models for the line and continuum, as described in §6). In order that the results can be used for future statistical analyses, statistical errors corresponding to 68% confidence for three interesting parameters ($\Delta C = 3.506$) are given. In addition, a more conservative measure, the 90% confidence, three-parameter range ($\Delta C = 6.251$) for each line parameter is also given in Table 1.

Table 1 shows that the peak energy of the Fe $K\alpha$ emission-line core is tightly constrained around 6.40 keV in all five observations, and shows no evidence for variability even at the 68% confidence level. The line intensity has 68% confidence statistical errors of the order of $\sim 30\%$ and also shows no sign of variability. The equivalent width (EW) however, ranging from $\sim 50 - 90$ eV, does show variability at the 68% confidence level, but not at the 90% confidence level. However,

any EW variability in this case is simply due to the continuum level changing whilst the line intensity remains steady. The 2–10 keV flux and luminosity show only $\sim 50 - 60\%$ variability over the entire monitoring campaign. The most interesting result from Table 1 is that in the first two observations the Fe K α line core appears to be resolved at the 90% confidence level, but in the latter three observations it appears to be unresolved. The 90% upper limit on the FWHM in the last three observations is not more than 3000 km s^{-1} , but for the first two observations it is 4000 km s^{-1} or more. For comparison, the FWHM resolution of the HEG at 6.4 keV is $\sim 1860 \text{ km s}^{-1}$.

We report the results of investigating this apparent variability of the width of the Fe K α line core further in §3.3, but first we report the results of investigating the dependence of the Fe K α core line parameters on the details of modeling the continuum and absorption.

3.2. Dependence of Fe K α Line Parameters on Continuum and Absorption Modeling

Here we use the ~ 830 ks MEG and HEG spectra (i.e. summed over the five observations) to investigate in detail the effect of using an over-simplified empirical continuum (as described above) on the derived Fe K α core line parameters. It is well known that there is a complex photoionized absorber in NGC 3783, with at least two components. The absorber has been modeled in great detail by several research groups, using *Chandra* and *XMM-Newton* data (e.g. Kaspi *et al.* 2002; Netzer *et al.* 2003; Krongold *et al.* 2003; Behar *et al.* 2003). Since highly ionized components of the absorber can affect the data even in the Fe-K band, it is conceivable that the warm absorber can affect interpretation of the broad part of the Fe K α emission line. In fact, the apparent lack of a *broad* Fe K α emission line in recent *XMM-Newton* data was attributed to the complex absorber not modeled adequately in previous analyses (Reeves *et al.* 2004). Reeves *et al.* (2004) also reported an absorption line due to He-like or H-like Fe in the same *XMM-Newton* data. We expect the effect of the photoionized absorber on the narrow Fe K α emission-line core to be unimportant, but since we will also be searching for spectral variability over a broader energy range than just the line core, and revisiting the question of the presence of a broad Fe K α line,

we constructed a model of the photoionized absorber.

We compiled a spectral energy distribution (SED) from the literature to use as an input to the photoionization code XSTAR², which was then used to construct grids of models for spectral fitting. Full details and results for the complex absorber modeling are given in McKernan, Yaqoob, & Reynolds (2005, MN, submitted). For the present purpose of Fe K α line modeling, we did not attempt to model the individual soft X-ray absorption-lines and features at the level of detail accomplished in the dedicated studies mentioned above. We found that a two-component absorber combined with a broken power-law continuum was sufficient to model the broadband MEG and HEG data. The model was derived by first fitting the MEG 0.5–7 keV data, using an additional Gaussian to model the Fe K α emission-line core, whose parameters were initially frozen at the values derived using the simple power-law continuum model (§3.1). Then this model was fitted to the 0.8–9 keV HEG data with all parameters except the hard X-ray slope frozen. Then, restricting the energy range to 2–7 keV (in order to directly compare derived emission-line parameters with the empirical continuum fits in §3.1) the Gaussian emission-line parameters (peak energy, width, and intensity) were allowed to float and the best-fit found. The photoionized absorber components had column densities of $4.7 \times 10^{21} \text{ cm}^{-2}$ and $3.5 \times 10^{22} \text{ cm}^{-2}$, with corresponding ionization parameters $\log \xi = 0.74$ and 2.21 respectively (where $\xi \equiv L_{\text{ion}}/n_e r^2$, L_{ion} being the 1–1000 Rydberg ionizing luminosity, n_e the electron density, and r the source to absorber distance). The soft X-ray modeling is discussed in detail in McKernan *et al.* (2005, MN, submitted), as well as in the several studies mentioned above so we do not discuss it any further. Fig. 2 (a) shows the ratio of the summed HEG data to this model in the 2–7 keV band, with the data binned at 0.005 \AA . The other five panels in Fig. 2 (b)–(f) show the ratio of the data, from each of the five snapshots, to this same model, with only the overall normalization adjusted to obtain the best-fit. Aside from line-like features between $\sim 6 - 7$ keV, the model gives a strikingly good fit to the spectra from all five of the separate observation data sets. We will address the possible origin of these

²<http://heasarc.gsfc.nasa.gov/docs/software/xstar/xstar.html>

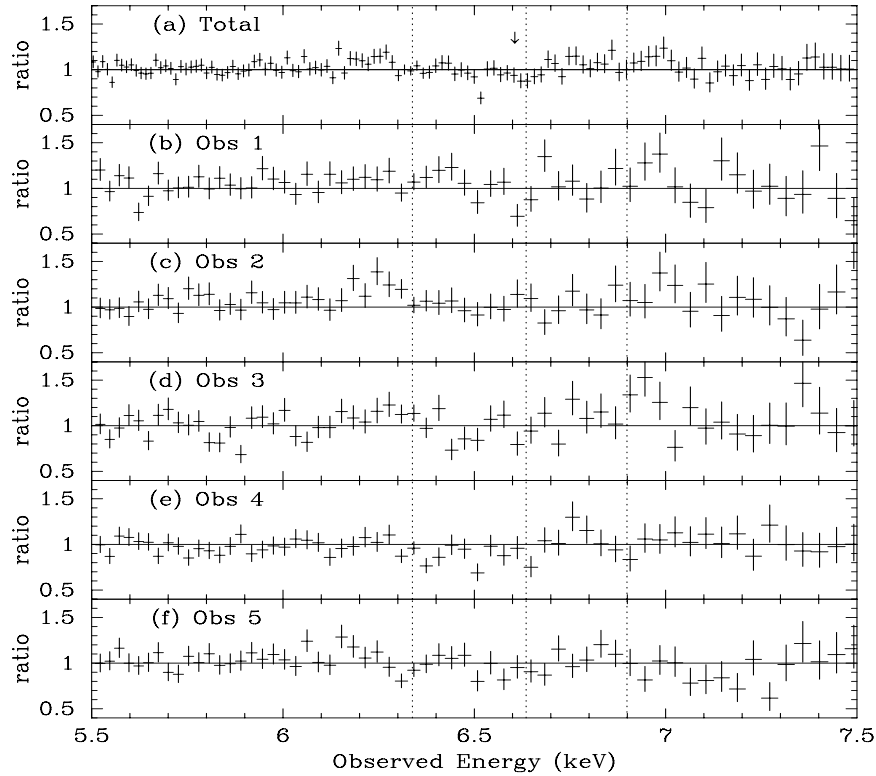


Figure 2. Ratios of data/model for the *Chandra* HEG data for NGC 3783. The model consists of a complex continuum plus warm absorber and simple Gaussian Fe $K\alpha$ emission line, fitted as described in §3.2, to the total ~ 830 ks HEG spectrum (i.e. all snapshots combined). The ratio of the total HEG spectrum, binned at 0.005\AA , to this model is shown in (a). The ratios of HEG spectra (for the individual snapshots binned at 0.01\AA) to exactly the same model (with all parameters fixed at the values obtained from fitting the total spectrum, apart from an overall renormalization) are shown in (b)–(f). Note that the bin size for the individual snapshot spectra in (b)–(f) is comparable to the HEG FWHM spectral resolution of $\sim 0.012\text{\AA}$. It can be seen that there is very little evidence for spectral variability, aside from line-like residuals between $\sim 6 - 7$ keV in some of the ratio plots. Vertical dashed lines indicate energies of 6.400 keV, 6.700 keV, and 6.966 keV in the NGC 3783 rest frame, corresponding to the energies of the Fe I $K\alpha$, Fe XXV $1s^2 - 1s2p$ (resonance), and Fe XXVI Ly α transitions. The arrow in (a) indicates the position in energy of the Fe-K absorption feature found in the *XMM-Newton* data by Reeves *et al.* (2004).

residuals in more detail in §6. The apparently variable line-like features at ~ 7 keV are likely to be due to Fe XXVI Ly α emission (which, blended with Fe $K\beta$, was detected in *XMM-Newton* data by Reeves *et al.* 2004; also see Kaspi *et al.* 2002).

Fig. 3 shows joint, two-parameter, 99% confidence contours directly comparing the derived Fe $K\alpha$ line results for the simple and complex continuum models. Black contours show the results using the simple, empirical power-law continuum, and red contours show the results using the warm absorber plus complex intrinsic continuum described above. Specifically, Fig. 3 (a) shows the Fe $K\alpha$ line intensity versus line center energy contours, whilst Fig. 3 (b) shows the EW versus FWHM contours. It can be seen that

although both the line intensity and EW are consistent at the 99% confidence level from the two different continua, the fits using a complex continuum give values for the best-fitting line intensity and EW which are $\sim 20\%$ higher than those obtained using the simple power-law continuum only. This is because the intrinsic flux from the line has to be larger to compensate for the absorption in the complex model. However, we do not in fact know whether the warm absorber lies farther from the X-ray continuum source than the Fe $K\alpha$ line emitter so there is an inherent uncertainty in the Fe $K\alpha$ line intrinsic intensity which will only be resolved when we are able to constrain the geometry of the system better with future missions (but see §5 and §6).

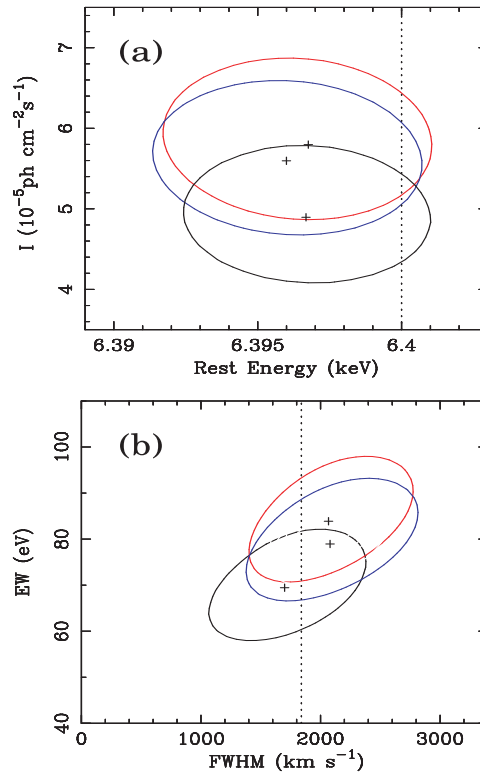


Figure 3. Joint, two-parameter, 99% confidence contours for the Fe K α emission-line core from the total, ~ 830 ks, *Chandra* HEG spectrum of NGC 3783, illustrating the effects of different levels of approximation in modeling the continuum. Black contours correspond to a simple power-law continuum (fitted in the 2–7 keV band), red contours correspond to a model including a photoionized absorber, as described in §3.2, and blue contours include a Compton-reflection continuum in addition to the photoionized absorber, also described in §3.2. The emission-line is modeled by a simple Gaussian and (a) shows the line intensity versus center energy, and (b) shows the line equivalent width (EW) versus FWHM. All quantities are in the rest frame of NGC 3783. It can be seen that the center energy of the line is not sensitive to details of modeling the continuum, but there is some model dependency on the line intensity, EW, and FWHM. However, the differences are not statistically significant at the 99% confidence level. The dotted line in (a) corresponds to the rest-energy of Fe I K α (6.400 keV) and the dotted line in (b) corresponds to the HEG FWHM resolution at the observed center energy of the Fe K α line.

The *Chandra* HEG data are not sensitive enough to strongly constrain a Compton-reflection continuum. However, we investigated the effect of including a Compton-reflection continuum (in addition to the complex ionized absorber model described above) since it is conceivable that it could still affect the derived line parameters as it has a complex shape in the 6–7 keV region due to the Fe-K edge. Moreover, if the Fe K α emission line is formed in optically-thick matter (for example reflection from the inner surface of a putative obscuring torus), a Compton-reflection continuum is *expected*. We used the PEXRAV model in XSPEC (see Magdziarz and Zdziarski 1995). Although this model is based on a disk geometry, it is adequate for our pur-

pose since the *Chandra* data are not sensitive to the differences in geometry. Again, since the data cannot constrain this model well, the parameters of the reflection model were fixed at nominal values (except for the photon index and normalization of the intrinsic power-law continuum). Specifically, we fixed the Fe abundance at the default solar value, the disk inclination angle at 30° , and the effective solid angle of the reflector at 2π (i.e. the “reflection factor”, $R = 1$). However, in §5 and §6 we will investigate the effect of allowing R to be free. The e-folding cutoff energy of the power law was fixed at 300 keV, well outside the range of the data.

Fig. 3 (a) shows the joint, two-parameter, 99% confidence contour (blue) of the Fe K α line inten-

sity versus line center energy, and Fig. 3 (b) shows the two-parameter, 99% confidence contour of the line EW versus FWHM. These contours are directly compared with the corresponding contours derived with the Compton-reflection continuum omitted (red), and with only a simple power-law (black). It can be seen that the effect of omitting the Compton-reflection continuum on the derived parameters of the core of the Fe K α emission line is negligible, even at the 99% confidence level. The effect of the ionized absorber on the line parameters is far more important.

3.3. Variability of the Fe K α Line Core

Fig. 4 (a) shows the joint, two-parameter, 99% confidence contours of the Fe K α line intensity versus center energy obtained from the time-averaged HEG spectrum (black) compared with those obtained from the five individual observations (or “snapshots”). This confirms the result from the spectral fitting (see Table 1), that at 99% confidence, the intensity and peak energy of the Fe K α line core do not vary.

The five snapshots span a range of timescales from < 2 days to ~ 125 days. However, long-term intensive monitoring of NGC 3783 with *RXTE*, some of which was simultaneous with the present *Chandra* observations, shows that the continuum varies significantly on all timescales in this range (Markowitz & Edelson 2004). Therefore all we can say is that the actual response time of the Fe K α line core must be greater than ~ 2 days because if the continuum varies more rapidly than the response time, the Fe K α line core intensity measured will correspond to some average continuum level. If we take $t > 169$ ks as the response time for the Fe K α line core to continuum variations, we get $r > 5 \times 10^{15}$ cm for the location of the line-emitter relative to the continuum source (the recombination timescale likely does not play a role here since the center energy of the Fe K α line core indicates neutral Fe). For a central black hole mass of $2.9 \times 10^7 M_\odot$ (Peterson *et al.* 2004), this corresponds to $r > 1000 r_g$, where $r_g \equiv GM/c^2$ is the gravitational radius. However, the FWHM of the Fe K α line core (~ 1700 km s $^{-1}$ from the total combined spectrum) places its origin much further from the central black hole. The actual width already indicates that it might coincide with the outer BLR/inner NLR. Note that in the present paper, all quoted line widths derived from spectral fitting are already corrected for the

instrumental line-spread function. Assuming a virial relation and an r.m.s. velocity dispersion of $\sqrt{3}v_{\text{FWHM}}/2$ (e.g. Netzer 1990), places the line emitter at 0.06 pc, or ~ 70 light days from the central continuum source (using the above mass). If some of the line width is not kinematic in origin (e.g. if there are multiple lines from different ionization states of Fe), then this distance is even greater. This is consistent with the lack of response of the line intensity to continuum variability. However, the lack of variability of the narrow Fe K α line core *is not necessarily an expected result*, because variability in the narrow Fe K α line core has been observed in Mkn 841 (Petrucchi *et al.* 2002), independent of the continuum (and that result is still not fully understood, but see Longinotti *et al.* 2004).

In §3.1 (Table 1) we showed that observations (1) and (2) appeared to have a somewhat broader Fe K α line core than observations (3)–(5). To investigate further, we combined the five HEG spectra into two groups, one spectrum from observations (1) and (2), and the other spectrum from observations (3)–(5). Fig. 4 (b) shows the joint, two-parameter, 68%, 90%, and 99% confidence contours of the Fe K α line EW versus the FWHM, for these two grouped spectra, compared with the 99% contour obtained from the mean, time-averaged spectrum. Indeed, the 68% confidence contours from observations (1) and (2) do not overlap with those from observations (3)–(5), the latter showing a narrower line width than the former, with the narrower line having a somewhat smaller flux than the broader line. Thus, at 68% confidence, the Fe K α line core appears to be broader and more intense in observations (1) and (2) than in observations (3)–(5). However, the 90% and 99% confidence contours *do* overlap so we cannot say that the line width varied at 90% confidence or greater. On the other hand, the line is resolved by the HEG at higher than 99% confidence in observations (1) and (2) but is not resolved at 99% confidence in observations (3)–(5). Future instrumentation will have to address the question of variability in the line width.

4. He-like Fe Absorption Feature

Kaspi *et al.* (2002) reported He-like Fe absorption in the *Chandra* HETGS data. Reeves *et al.* (2004) detected the absorption line from an *XMM-Newton* observation of NGC 3783 (in

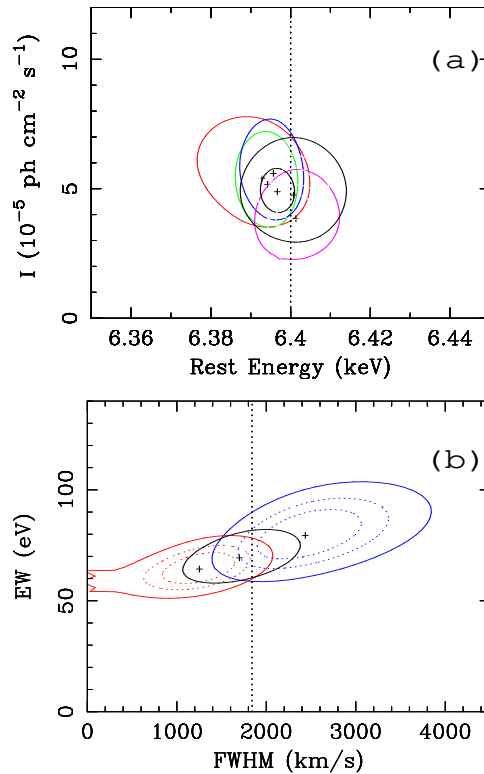


Figure 4. (a) Joint, two-parameter, 99% confidence contours of line intensity versus center energy (both in the AGN rest frame) for the Fe K α emission-line core (modeled with a simple Gaussian) from *Chandra* HEG spectra of NGC 3783. The continuum was modeled by a simple power-law, fitted over the 2–7 keV energy range. The small, black contour was obtained from the total, ~ 830 ks, HEG spectrum. Remaining contours were obtained from the individual snapshots as follows: black (large), observation (1); red, observation (2); green, observation (3); blue, observation (4); magenta, observation (5). See §3 for details. It can be seen that there is no discernible variability at the 99% confidence level. The dotted line is at 6.400 keV in the rest frame of NGC 3783. (b) Joint, two-parameter, confidence contours of line equivalent width (EW) versus line FWHM (both in the AGN rest frame) for the Fe K α emission-line core in the NGC 3783 HEG data, using the same model as in (a). Black contour shows the 99% confidence region for the total, ~ 830 ks, HEG spectrum. Remaining contours were obtained by combining the snapshots from observations (1) and (2) (blue contour), and observations (3), (4), and (5) (red contour). Dotted lines show the 68%, and 90% confidence regions and solid lines show the 99% confidence contours. These combinations were formed after examining the contours of all five observations separately and grouping them according to similar widths. It can be seen that there is marginal evidence for a change in the effective width of the line, which appears to be resolved in observations (3), (4) and (5), but not in observations (1) and (2) (the dotted line corresponds to the HEG FWHM resolution at the observed center energy of the line).

December 2001), centered at 6.67 ± 0.04 keV (in the source rest frame), with an EW of 17 ± 5 eV. The line was attributed to Fe XXV $1s^2 - 1s2p$ resonance absorption and it was not resolved by the CCDs. Evidence for this absorption feature can be seen in Fig. 2 (an apparent absorption dip is indicated by an arrow). We modeled the feature by adding an inverted Gaussian to the two-component warm absorber plus broken power-law model described in §3 (including the Gaussian emission line). All parameters except for the hard power-law slope, the overall continuum normalization, and the three absorption-line parameters (center energy, intrinsic width) were frozen

at their best-fitting values. The C -statistic decreased by 9.2 upon the addition of the absorption line, which corresponds to a detection significance of only 99% for three additional free parameters. For the line center energy, EW, and intrinsic width, we measured $6.62^{+0.07}_{-0.06}$ keV, 12^{+8}_{-7} eV, and 6405^{+5020}_{-2670} km s $^{-1}$ FWHM respectively (errors are one-parameter, 90% confidence, to facilitate direct comparison with the *XMM-Newton* results of Reeves *et al.* 2004). Thus, the *Chandra* HETGS and *XMM-Newton* measurements are consistent with each other.

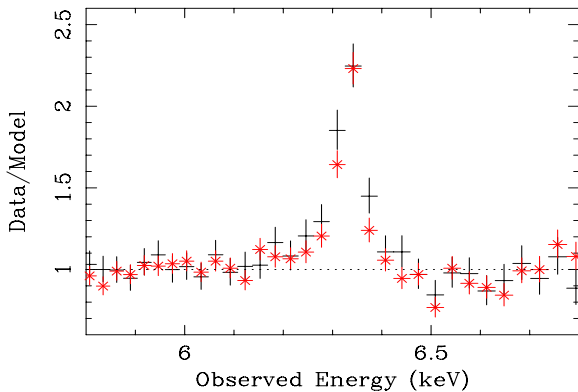


Figure 5. Ratios of HEG data for NGC 3783 to a simple power-law continuum model, fitted in the 5–7 keV band, omitting the 6.0–6.5 keV data. Black data points correspond to the summed spectra from observations (1) and (2), and the red data points correspond to the summed spectra from observations (3), (4), and (5). These two groupings show similar line widths within each group, from examination of the data from the individual observations (see Fig. 4 and §3). This direct comparison shows how the Fe K α line core is slightly broader in observations (1) and (2) (black) than in observations (3), (4), and (5) (see Fig. 4). The continuum was fitted to the two data sets simultaneously, with the photon index tied together. Although the continuum is over-simplified, the purpose here is simply to compare the emission-line core for the two data sets.

5. Fe K α Line Compton Shoulder

Using the same NGC 3783 *Chandra* HEG data as described in the present paper, Kaspi *et al.* (2002) noted the detection of a so-called “Compton shoulder” on the red side of the peak of the Fe K α emission line. This structure would be due to the core Fe K α emission-line photons Compton-scattering on electrons in the medium in which the line is formed, before escaping the medium and reaching the observer. If the material in which the line is formed is not too hot (i.e. $kT \ll 6.4$ keV), the Compton scattering results in the line photons losing energy so that the scattered emission appears redward of the peak of the line. The relative magnitude of the Compton shoulder relative to the peak line flux increases with optical depth of the medium, until the medium becomes optically-thick (see, for example, Matt 2002, for a theoretical description and Monte Carlo calculations). The peak of the once-scattered photon energy distribution is ex-

pected at two Compton wavelengths longer than the wavelength of the unscattered line photons. For a line at 6.4 keV, this is ~ 6.25 keV in the rest frame of NGC 3783, or 6.19 keV in the observed frame. The excess flux to the red side of the Fe K α line core can be seen in Fig. 2 (a) and Fig. 5 and does in fact appear to extend down to the appropriate energy.

We applied a model of the Compton shoulder to the NGC 3783 HEG data. For the line scattering we used the XSPEC model of Watanabe *et al.* (2003). The intrinsic width of the emission line in this model is much less than the instrument resolution and includes no kinematic information so is rather unphysical. During preliminary fitting we found that the model always left excess flux blueward of the Fe K α line core. Therefore we convolved the line profile with a Gaussian whose width was a free parameter, in order to mimic Doppler broadening of the intrinsic line profile. We used the broken power-law plus two-component warm absorber, with a Compton-reflection continuum as the baseline model, as described in §3.2. The parameters of the warm absorber and Compton reflection models were fixed at the values described in §3.2. The fitting was performed between 2–9 keV (i.e. the high-energy end of the fitted range was now extended from 7 keV up to 9 keV). Only the hard X-ray slope, the overall continuum normalization, and the column density of the Compton-scattering medium were free parameters. Since the Fe K α line peak energy indicates low ionization states of Fe and is consistent with Fe I, the temperature of the scattering medium must be low and we assumed the medium is neutral (“cold”). The data, best-fitting model, and data/model ratio are shown in Fig. 6 (a). Note that the He-like Fe absorption line discussed in §4 has deliberately not been modeled in Fig. 6 (a) in order to clearly show its presence and magnitude, especially in the data/model ratios, and to facilitate comparison with the *XMM-Newton* data. We obtained a FWHM of 1500^{+460}_{-340} km s $^{-1}$ for the width of the Gaussian used to convolve the Compton-scattered line profile. The column density we derived was $7.5^{+2.7}_{-0.6} \times 10^{23}$ cm $^{-2}$ (90%, one-parameter errors). This corresponds to a Thomson depth of ~ 0.60 , which is not quite Compton-thick. The Thomson depth of the scattering medium must be less than $\sim \sqrt{2}$, or else the mean number of scatterings would be ~ 2 and the peak energy of

the scattered photons would be much lower than measured (the scattered line photons would have a distribution with significant flux down to four Compton wavelengths below the zeroth-order line peak). A Thomson depth of $\sqrt{2}$ corresponds to $\sim 1.7 \times 10^{24} \text{ cm}^{-2}$.

Ideally, we would self-consistently model the Compton-reflection continuum and the Compton-scattered line since both are produced by the same physical process. When we allowed the relative normalization of the Compton reflection continuum, R , to be a free parameter, we obtained $R = 1.0^{+0.5}_{-0.3}$ (justifying $R = 1$ in the fits thus far). However, the Compton-reflection continuum model is calculated for an optically-thick disk, but the emission line may be produced in transmission since we measured a small Thomson depth from the Compton shoulder. Better data are required to justify more sophisticated modeling.

6. Relativistic Disk Line Model

We investigated whether a relativistically broadened Fe K α line (in addition to a narrow Gaussian component) could also account for the Fe K α line profile in NGC 3783. We fitted the 2–9 keV HEG data using a broken power-law plus two-component warm absorber, with a Compton-reflection continuum as the baseline model, as described in §3.2. Initially, the Compton-reflection parameter, R , was fixed at unity, which corresponds to the expected steady-state normalization of the reflected continuum from a neutral (“cold”) Compton-thick disk subtending a solid angle of 2π at the X-ray source. Preliminary spectral fitting with R free showed that the best-fitting value is $R \sim 1$ in any case (as in §5), and we will give statistical errors when R was a free parameter below. In addition to the above model components we included a Gaussian (to model the line core), and an emission line from a relativistic disk around a Schwarzschild black hole (e.g. see Fabian *et al.* 1989). The energy, intrinsic width, and intensity of the Gaussian were free parameters. The inner radius of line emission from the disk was initially fixed at $6r_g$ ($r_g \equiv GM/c^2$) and the outer radius was fixed at $1000r_g$. The line radial emissivity was assumed to be a power law (line emissivity proportional to r^{-q}), with the index, q , free. In the disk rest-frame the emission-line energy was fixed at 6.4 keV. The disk inclination angle and overall line intensity were also

free parameters. Thus, there were a total of seven free parameters for this model, including the continuum slope and normalization.

The data, best-fitting model, and data/model ratio are shown in Fig. 6(b). It can be seen that the fit is as good as that for the Compton-scattering model, shown in Fig. 6(a). Again, we deliberately did not model the He-like Fe absorption feature discussed in §4 in order to clearly show its effect and to facilitate comparisons between *Chandra* and *XMM-Newton* data. In the 5.7–6.9 keV energy band shown in the figure, the C -statistic for the disk-line model is less than that for the Compton shoulder model (§5) by only 1.6 for an additional three free parameters. Thus, although the disk-line model is not statistically preferred over the Compton shoulder model, it cannot be ruled out. The center energy of the Gaussian was 6.399 keV, with statistical errors similar to those obtained from simpler continuum models (Table 1). Since the peak energy was well-determined, this parameter was fixed when deriving the statistical errors for the other parameters in the model (in this section, all errors are 90% confidence, one-parameter, or $\Delta C = 2.706$). The Gaussian line FWHM obtained was $1460^{+470}_{-680} \text{ km s}^{-1}$. The Gaussian line width was then fixed at the best-fitting value in order to derive statistical errors on the remaining model parameters, in order to avoid the spectral fitting becoming unstable.

We obtained EWs of $56^{+14}_{-11} \text{ eV}$ and $39^{+18}_{-16} \text{ eV}$ for the Gaussian and disk emission-line components respectively (all line measurements are in the source frame). The radial emissivity index measured for the disk-line emission was $q = 1.90^{+0.63}_{-0.57}$, and the inclination angle was constrained with an upper limit only, of 11° . When we allowed the relative normalization of the Compton-reflection continuum, R , to be a free parameter we obtained $R = 1.0^{+0.4}_{-0.3}$. We recall that $R = 1$ corresponds to the case of time-steady illumination of a thick disk subtending 2π solid angle at the X-ray source. We note that De Rosa *et al.* (2002) obtained $R = 0.71^{+0.20}_{-0.28}$ from non-contemporaneous *BeppoSAX* data for NGC 3783, and Markowitz, Edelson, & Vaughan (2003) obtained $R = 0.62 \pm 0.12$ from *RXTE* data which overlapped with the first three *Chandra* observations reported in the present paper, consistent, within the errors, with the *Chandra* value. However, Markowitz *et al.* (2003) also reported $R =$

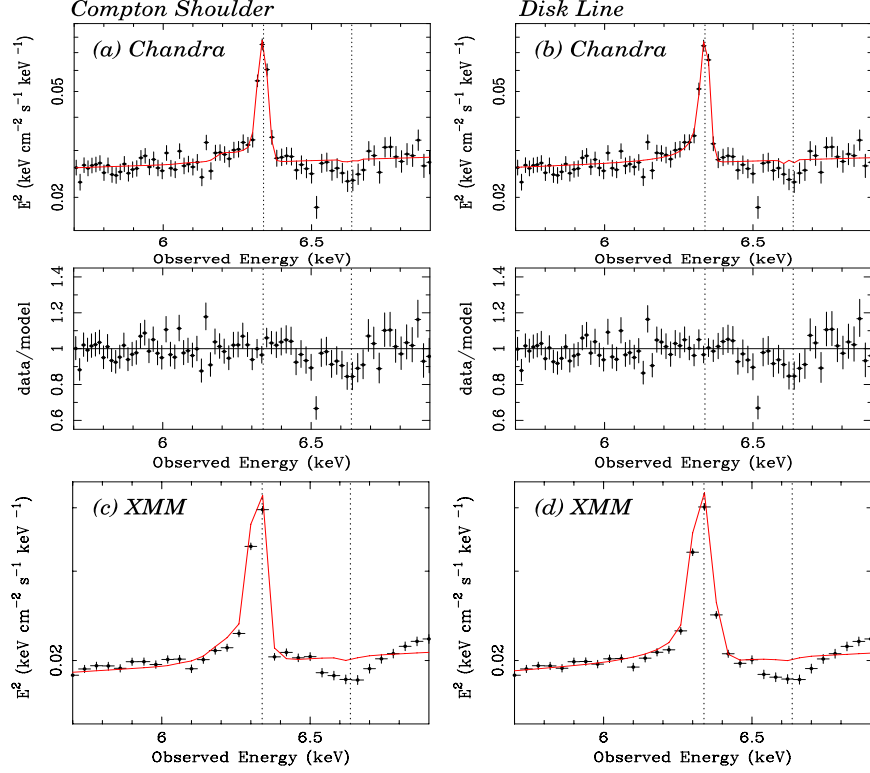


Figure 6. (a) Modeling of the Compton shoulder of the Fe K α line in the total, ~ 830 ks, *Chandra* HEG spectrum of NGC 3783 (the data are binned at 0.005\AA for the plot). The model consists of a power law, photoionized absorber, a Compton-reflection continuum, and a narrow Fe K α line which suffers Compton scattering in cold, solar-abundance material, observed in transmission. The line profile was convolved with a Gaussian, whose best-fitting width was 1500^{+460}_{-340} km s $^{-1}$. See §5 for details of the fitting procedure and results. (b) The *Chandra* HEG spectrum, same as in (a), fitted with an emission line profile from a relativistic accretion disk rotating about a Schwarzschild black hole, plus a Gaussian to model the Fe K α line core. See §6 for model-fitting details and results. Note also that the dip at ~ 6.51 keV (observed frame) is not real: it is narrower than the instrument resolution (0.012\AA FWHM) and is not detected in *both* the -1 and $+1$ orders of the grating. (c) The *Chandra* Compton-shoulder model in (a) fitted to non-contemporaneous *XMM-Newton* EPIC pn CCD data for NGC 3783, with only the overall normalization and power-law slope free. (d) The *Chandra* disk line plus Gaussian model in (b) fitted to non-contemporaneous *XMM-Newton* pn data for NGC 3783, with only the overall normalization and power-law slope free. See Reeves *et al.* (2004) for details of the *XMM-Newton* data. We note that all of the line profiles shown here are *not* unfolded: the profiles correspond to the ratio of counts to predicted model counts, multiplied by the best-fitting model. Note that the absorption line at ~ 6.7 keV was deliberately *not* modeled for any of the four cases shown here, in order that the reader can readily compare the absorption line in the *Chandra* and *XMM-Newton* data. See §4 or Reeves *et al.* (2004) for detailed fitting of the absorption line in the *Chandra* or *XMM-Newton* data respectively.

$0.47^{+0.05}_{-0.04}$ for *RXTE* data taken over a ~ 3.2 year period between 1999–2002. Over such a long timescale variability can obviously be a factor responsible for the smaller value of R .

Upon allowing the outer disk radius to be a free parameter in the original disk model, with R fixed at 1.0, we obtained a lower limit on its value of $\sim 540r_g$. The inner disk radius and q are correlated in the sense that they affect the overall width of the emission line: larger inner radii allow steeper radial emissivity index (q) since the part of the disk giving the broadest part of the line with a steep q would then be missing. The data do not allow the ambiguity between q and the

inner radius to be removed. By examining confidence contours of q versus r_{in} , we found that a radial emissivity steeper than even r^{-3} is allowed if r_{in} is of the order of $100r_g$ or larger.

We note that our results for the relativistic disk line are *not* inconsistent with the findings of Reeves *et al.* (2004), namely that the *XMM-Newton* data do not *require* a disk line when the warm absorber is taken into account. Reeves *et al.* (2004) obtained a 90% upper limit on the EW of a disk line of 35 eV. However, this assumed a steep emissivity index ($q = 3$) combined with a small inner disk radius ($r_{\text{in}} = 6r_g$), and a disk inclination angle of 30° . With a flatter emissivity

and a smaller inclination angle, as obtained from the *Chandra* HEG data, a larger EW is allowed because the disk line width is narrower. Thus, the *Chandra* HEG and *XMM-Newton* measurements are consistent with each other. The reason why the *XMM-Newton* data do not yield a significant detection of the disk line is that the *Chandra* HEG data are more sensitive to a *narrow disk line*, due to the factor of ~ 4 better spectral resolution. In Fig. 6 (c) and Fig. 6 (d), we show that both the best-fitting *Chandra* HEG Compton-shoulder model and disk-line model respectively, fit the *XMM-Newton* data equally well. For fitting the *XMM-Newton* data (the same data as in Reeves *et al.* 2004, which were taken at a different time to the *Chandra* data), all parameters except the overall normalization and the power-law slope were fixed at their *Chandra* best-fitting values. Again, the He-like Fe absorption feature discussed in §4 was deliberately not modeled here in order to facilitate comparison between the *Chandra* and *XMM-Newton* data.

Although Fe $K\beta$ line emission is expected to accompany Fe $K\alpha$ line emission, the HEG data are not so sensitive to Fe $K\beta$ lines because the branching ratio is 17:150 for $K\beta : K\alpha$. Having said that, line-like residuals are apparent in the spectral ratios shown in Fig. 2 but some part of this line emission could be due to Fe XXVI Ly α . Reeves *et al.* (2004) reported significant line emission at ~ 7 keV from *XMM-Newton* data and obtained an EW of 20 ± 5 eV for Fe XXVI Ly α after accounting for Fe $K\beta$ emission. Since Fe $K\beta$ line emission is *expected* to accompany the Fe $K\alpha$ line emission, we self-consistently added Gaussian and disk-line Fe $K\beta$ emission with the expected branching ratio to the Gaussian plus disk-line model described above in order to test the *Chandra* HEG data for Fe XXVI Ly α emission. We modeled the latter with an additional Gaussian, fixing the energy at 6.966 keV (e.g. see Pike *et al.* 1996) but leaving the intrinsic width free for the summed, ~ 830 ks HEG spectrum, but fixing it at the resulting best-fit value for the individual spectra from observations (1)–(5). The best-fitting intrinsic width from the summed HEG spectrum was 9200 km s^{-1} FWHM. However, we did not obtain a very significant detection (ΔC was always less than 2.7) for either the summed spectrum (90%, one-parameter upper limit: 17 eV) or the individual spectra from the five observations. Although Fig. 2 shows evidence of variability of

the line-like residuals at ~ 7 keV, we could only obtain upper limits on the EW (29, 27, 65, 41, and 14 eV for observations (1), (2), (3), (4) and (5) respectively). All of the values of the Fe XXVI Ly α EW upper limits we obtained are consistent with the EW measurements from *XMM-Newton* data by Reeves *et al.* (2004).

7. CONCLUSIONS

We have presented results of X-ray spectroscopy of the Fe-K line region in NGC 3783 from an extended monitoring campaign with the *Chandra* High Energy Grating Transmission Spectrometer (*HETGS*). Consistent with previous studies, the Fe $K\alpha$ line core is resolved in the time-averaged spectrum by the High Energy Grating (HEG) and has a center energy indicating an origin in neutral or lowly-ionized Fe. Despite a factor of ~ 1.5 variation in the X-ray continuum luminosity, we measured no variability in the intensity of the Fe $K\alpha$ line core during five observations comprising the observing campaign, over ~ 125 days. The lack of response to the continuum is consistent with the fact that a virial interpretation of the line FWHM ($\sim 1700 \text{ km s}^{-1}$) gives a distance between the putative central black hole and the line emitter of at least 0.06pc, or 70 light days. However, we detected marginal evidence for variability in the intrinsic width of the Fe $K\alpha$ line core. In two out of the five snapshots the Fe $K\alpha$ line was resolved and had a FWHM of $\sim 2300 \text{ km s}^{-1}$, whilst in the other three snapshots the line was unresolved. This apparent variability was not related to the X-ray continuum level. At 68% confidence, the Fe $K\alpha$ line core was broader and had a higher flux in the first two ~ 170 ks snapshots than in the last three. If the line width variability is real it could be due to changes in the matter distribution and/or ionization state as a function of distance from the central engine and would be important to investigate with future missions.

We found that the excess flux around the base of the Fe $K\alpha$ line core can be modeled by an emission line from a relativistic disk rotating around a black hole, as well as a model in which line core photons are Compton-scattered (forming a “Compton shoulder” on the red side of the line peak). More realistic modeling should self-consistently include Compton-scattering of line photons, whether the line photons originate in an

optically-thick disk or more distant matter. Also, the Compton-scattered continuum should be self-consistently computed. In principle, measurement of the unscattered and scattered line photons, along with the reflected continuum, would constrain whether the core of the Fe $K\alpha$ line originates in optically-thick matter (such as the putative obscuring torus) or in optically-thin matter (e.g. the BLR and/or NLR). However, the signal-to-noise of the current data is not sufficient to distinguish between these scenarios. We note that a Compton shoulder has not been detected in any other *Chandra HETGS* observation of a Seyfert 1 galaxy (Yaqoob & Padmanabahn 2004). If this is verified by higher signal-to-noise data, it would suggest that the Fe $K\alpha$ line core is in general likely to originate in optically-thin matter. In the case of NGC 3783, the EW of the Fe $K\alpha$ line core deduced from the composite Gaussian plus disk-line model can easily be produced by optically-thin matter with $N_H \sim 10^{23} \text{ cm}^{-2}$, covering less than half the sky (e.g. see Yaqoob *et al.* 2001).

Modeled with a relativistic disk line, the disk inclination angle was constrained to be less than 11° and the emission line flux from the disk is comparable to that in the Fe $K\alpha$ line core. The disk-line modeling included a continuum with a complex photoionized absorber and Compton reflection modifying the intrinsic continuum. We showed that the *Chandra* HEG data are consistent with the *XMM-Newton* data in the sense that the same disk-line model can account for both data sets, even with these continuum complexities. Of course, with the current data it is not possible to rule out more complicated scenarios involving, for example, a disk line modified by Compton scattering, as mentioned above. We also confirmed previous detections (*HETGS*: Kaspi *et al.* 2002; *XMM-Newton*: Reeves *et al.* 2004) of an absorption feature in the Fe-K band (at $6.67 \pm 0.04 \text{ keV}$, and with an EW of $17 \pm 5 \text{ eV}$), likely to be due to He-like Fe absorption. On the other hand, evidence for Fe XXVI $\text{Ly}\alpha$ emission was marginal in the HEG data.

Future observations with higher spectral resolution, as afforded by *Astro-E2*, will be able to resolve important ambiguities remaining in the Fe-K band in NGC 3783. In particular, it will be possible to determine if the Fe $K\alpha$ line core is composed of more than one line component and to determine if the broad part of the Fe $K\alpha$ line is really due to a relativistic disk.

The authors thank Ian George, Jane Turner, Barry McKernan, and Shai Kaspi for valuable discussions, and S. Watanabe for use of his Comptonized line model. T.Y. gratefully acknowledges support from NASA grants NNG04GB78A, NAG5-10769, and AR4-5009X, the latter issued by the Chandra X-ray Observatory Center, which is operated by the Smithsonian Astrophysical Observatory for and on behalf of NASA under contract NAS8-39073. This research made use of the HEASARC online data archive services, supported by NASA/GSFC. This research has made use of the NASA/IPAC Extragalactic Database (NED) which is operated by the Jet Propulsion Laboratory, California Institute of Technology, under contract with NASA. The authors are grateful to the *Chandra* instrument and operations teams for making these observations possible.

REFERENCES

1. Arnaud, K. A. 1996, *Astronomical Data Analysis Software and Systems V*, eds. Jacoby, G., & Barnes, J., ASP Conference Series, Vol. 101, p. 17
2. Behar, E., Rasmussen, A. P., Blustin, A. J., Sako, M., Kahn, S. M., Kaastra, J. S., Branduardi-Raymont, G., & Steenbrugge, K. C. 2003, *ApJ*, 598, 232
3. De Rosa, A., Piro, L., Fiore, F., Grandi, P., Maraschi, L., Matt, G., Nicastro, F., & Petrucci, P. O. 2002, *A&A*, 387, 838
4. Fabian, A. C., Iwasawa, K., Reynolds, C. S., & Young, A. J. 2000, *PASP*, 112, 1145
5. Fabian, A. C., Rees, M. J., Stella, L., & White, N. E. 1989, *MNRAS*, 238, 729
6. Gabel, J. R. *et al.* 2003a, *ApJ*, 583, 178
7. Gabel, J. R. *et al.* 2003b, *ApJ*, 595, 120
8. Gehrels, N. 1986, *ApJ*, 303, 336
9. Kaspi, S., *et al.* 2001, *ApJ*, 554, 216
10. Kaspi, S., *et al.* 2002, *ApJ*, 574, 643
11. Krongold, Y., Nicastro, F., Elvis, M., Brickhouse, N. S., Liedahl D., & Mathur, S., 2003, *ApJ*, 597, 832
12. Lee, J. C., Iwasawa, K., Houck, J. C., Fabian, A. C., Marshall, H. L., & Canizares, C. R. 2002, *ApJ*, 570, L47
13. Longinotti, A. L., Nandra, K., Petrucci, P. O., & O'Neill, P. M. 2004, *MN*, 355, 929
14. Lubiński, P., & Zdziarski, A. A. 2001, *MNRAS*, 323, L37
15. Markert, T. H., Canizares, C. R., Dewey, D., McGuirk, M., Pak, C., & Shattenburg, M. L. 1995, *Proc. SPIE*, 2280, 168
16. Magdziarz, P., & Zdziarski, A. A. 1995, *MN*, 273, 837
17. Markowitz, A., Edelson, R., & Vaughan, S. 2003, *ApJ*, 598, 935
18. Markowitz, A., & Edelson, R. 2004, *ApJ*, 617, 939
19. Matt, G. 2002, *MN*, 337, 147
20. Nandra, K., George, I. M., Mushotzky, R. F., Turner, T. J., & Yaqoob, T. 1997, *ApJ*, 477, 602
21. Netzer, H. 1990, in *Active Galactic Nuclei*, ed. R. D. Blandford, H. Netzer, & L. Woltjer (Berlin: Springer), 137
22. Netzer, H., *et al.* 2003, *ApJ*, 599, 933
23. Pike, C. D., *et al.* 1996, *ApJ*, 464, 487
24. Perola, G. C., Matt, G., Cappi, M., Fiore, F., Guainazzi, M., Maraschi, L., Petrucci, P. O., & Piro, L. 2002, *A&A*, 389, 802
25. Peterson, B. M. *et al.* 2004, *ApJ*, 613, 682
26. Petrucci, P. O., *et al.* 2002, *A&A*, 388, L5
27. Reeves, J. N. 2003, in *ASP Conf. Ser., Active Galactic Nuclei, from Central Engine to Host Galaxy*, ed. S. Collin, F. Combes & I. Shlosman, (San Francisco: ASP), Vol. 290, 35
28. Reeves, J. N., Nandra, K., George, I. M., Pounds, K. A., Turner, T. J., Yaqoob, T. 2004, *ApJ*, 602, 648
29. Reynolds, C. S., & Nowak, M. A. 2003, *Phys. Rep.*, 377, 389
30. Sulentic, J. W., Marziani, P., Zwitter, T., Calvani, M., & Dultzin-Hacyan, D. 1998, *ApJ*, 501, 54
31. Turner, T. J., George, I. M., Nandra, K., & Turcan, D. 1999, *ApJ*, 524, 667
32. Turner, T. J., Kramer, S. B., & Reeves, J. N. 2004, *ApJ*, 603, 62
33. Watanabe, S. *et al.* 2003, *ApJ*, 597, L37
34. Weaver, K. A., Gelbord, J., & Yaqoob, T. 2001, *ApJ*, 550, 261
35. Yaqoob, T., George, I. M., Nandra, K., Turner, T. J., Serlemitsos, P. J., & Mushotzky, R. F. 2001, *ApJ*, 546, 759
36. Yaqoob, T., George, I. M., Kallman, T. R., Padmanabhan, U., Weaver, K. A., & Turner, T. J. 2003a, *ApJ*, 596, 85
37. Yaqoob, T., McKernan, B., Kramer, S. B., Crenshaw, D. M., Gabel, J. R., George, I. M., & Turner, T. J. 2003b, *ApJ*, 582, 105
38. Yaqoob, T., Padmanabhan, U., Dotani, T., & Nandra, K. 2002, *ApJ*, 589, 487
39. Yaqoob, T., & Padmanabhan, U. 2004, *ApJ*, 604, 63